Virus Genes (2019) 55:448–457
https://doi.org/10.1007/s11262-019-01672-0

ORIGINAL PAPER

Variability in the 3′ untranslated regions of the genomes of the different tick-borne encephalitis virus subtypes

Vladimir A. Ternovoi[1] · **Anastasia V. Gladysheva**[1,2] · **Eugenia P. Ponomareva**[1] · **Tamara P. Mikryukova**[1] · **Elena V. Protopopova**[1] · **Alexander N. Shvalov**[1] · **Svetlana N. Konovalova**[1] · **Eugene V. Chausov**[1] · **Valery B. Loktev**[1,2,3]

Received: 10 January 2019 / Accepted: 14 May 2019 / Published online: 20 May 2019

Abstract

Tick-borne encephalitis viruses (TBEVs) are usually divided into three major subtypes: European (TBEV-Eu), Siberian (TBEV-Sib) and Far Eastern (TBEV-FE). The TBEV-Eu strains have the longest genomes, and TBEV-FE strains have the smallest genomes. Changes in the variable region of the untranslated region (V3′ UTR) play a major role in determining the viral genome length. Analyses of the 3′ UTRs of the different subtypes of TBEV have revealed significant changes in the secondary structures of the V3′ UTR of TBEV. More complex secondary structures of the V3′ UTR regions are typical for TBEV-Eu. The Siberian strain Tomsk-PT122 was isolated from birds and has an unusual 3′ UTR. Several short fragment (24–26 nucleotides) insertions derived from the viral E (2) and NS4a (1) genes have been found in the V3′ UTR of Tomsk-PT122. Additionally, the length of the V3′ UTR increases from 21 to 37 nucleotides during passages of the C11-13 strain of TBEV-Sib into PEK, 293 and Neuro-2a cells. The elongation of the V3′ UTRs of Tomsk-PT122 and C11-13 is the first direct evidence of an intragenomic 3′ UTR modification (insertion) for TBEV. Thus, the obtained results suggest that changing the length of the V3′ UTR in the genome is typical for different TBEV subtypes and can play an essential role in effective TBEV replication in different host cells.

Keywords Flavivirus · Tick-borne encephalitis virus · Viral genome · 3′ UTR · Nucleotide sequence

Introduction

Flaviviruses (family Flaviviridae, genus *Flavivirus*) are conventionally divided into several large groups as follows: mosquito-borne flaviviruses (MBFV), tick-borne flaviviruses (TBFV), flaviviruses with unknown vectors of transmission and mosquito-only flaviviruses (without a known vertebrate host) [1]. The flavivirus virion (~ 50 nm) contains nucleocapsids that consist of protein C and positive single-stranded RNA (~ 11,000 n), which is surrounded by a lipid membrane and modified structural viral proteins E and M [2]. The flaviviral genomic RNA is flanked by the 5′ and 3′ untranslated regions (UTRs) that are crucial to initiate viral replication [3, 4]. The 5′ UTR and the 3′ UTR form secondary structures (stem-loops and Y-shaped structures) that are cis-acting elements for the replication, translation and packaging of the genome.

Two different models of the 3′ UTR secondary structure of genomic RNA have been predicted for flaviviruses using computer modelling [5, 6]. The first model was made independently from the 5′ UTR, and this model predicted the structure of the 3′ UTR to be a linear plot that includes stem-loop structures. Another model of the secondary structure of 3′ UTR flaviviruses is known as the cyclization model and was confirmed experimentally. It involves the interaction between the complementary sequences of the 3′ UTR and the 5′ UTR, which leads to the formation of regions with double-stranded viral RNA [7]. The most conservative sequence of the 3′ UTR

Edited by Joachim Jakob Bugert.

✉ Valery B. Loktev
valeryloktev@gmail.com; loktev@vector.nsc.ru

[1] Department of Molecular Virology for Flaviviruses and Viral Hepatitis, State Research Center for Virology and Biotechnology “Vector”, Koltsovo, Novosibirsk Region 630559, Russia

[2] Novosibirsk State University, Novosibirsk 630090, Russia

[3] Institute of Cytology and Genetics, Novosibirsk 630090, Russia

is a terminal 3′ LSH (long stable hairpin) with a short hairpin SL2 (stem-loop). The 3′ LSH region contains the five conserved nucleotides CACAG, and the crucial role of viral infectivity has been demonstrated. In all likelihood, the 3′ LSH interacts with the viral and cellular proteins of the polymerase complex, thus initiating effective viral genome replication. The 3′ LSH for all flaviviruses is located within LRS1 and LRS2 (long repeat sequence). The two Y-shaped structures of the conserved region of the 3′ UTR (C3′ UTR) are actually located in LRS2 and LRS3. The infectivity of TBFV and dengue virus is reduced by deletions near LRS2/LRS3 [8, 9]. It is hypothesized that these flaviviral RNA structures could have occurred from a duplicate "ancient" LRS that was conserved only for the TBFV group. The preservation of a redundant plot corresponding to LRS3 or LRS4 most likely occurred several times [10].

The secondary structures of RNA located proximally from the 3′ LSH-SL2 are different and typical for MBFV and TBFV [11]. Therefore, "dumbbell" (DB) DB1/DB2 and Y-shaped structures were also found in the 3′ UTRs of flaviviruses with unknown vectors [12]. The Y-shaped RNA structure is necessary for the replication of viral genomes, and this has been supported by experimental data [9, 13, 14].

Tick-borne encephalitis virus (TBEV) is the causative agent of tick-borne encephalitis, which is usually transmitted to humans by Ixodes ticks [2]. Based on their geographical prevalence and a phylogenetic analysis, TBEV has been classified into the following three main subtypes: European (TBEV-Eur), Siberian (TBEV-Sib) and Far Eastern (TBEV-FE) [15]. The mortality rate for TBEV-Eur subtype infections is relatively low (1–2%), whereas for TBEV-FE, it is approximately 30% [2]. Members of these three subtypes have differences in the nucleotide sequences of their polyproteins (up to 18%) and in their UTRs [16–18]. The average level of homology of the 5′ UTR of TBEV in the individual ticks was 95% for TBEV-FE and 89% for TBEV-Sib [14]. The virulence of TBEV is associated with viral RNA conformation in the variable region of the 3′ UTR [19, 20]. Additionally, the cellular host proteins interact with the 3′ UTR of TBEV genomic RNA [21].

This work was devoted to studying the structural organization of the 3′ UTR of the viral genome for the three main subtypes of TBEV, the 3′ UTR modification of C11-13 TBEV during experimental adaptation to three types of cells, the V3′ UTR elongation of Tomsk-PT122 isolated from birds and the changing of the 3′ UTRs of TBEVs as a possible factor for TBEV evolution in nature.

Materials and methods

TBEV strains and cells

Absettarov, Kolarovo-2008, Tomsk–PT122, Zausaev, Vasilchenko, Lesopark11, Buzuuchuk, Glubinnoe/2004, 4072, 205, Sofjin, Tomsk-PT12, Tomsk-PT14, Tomsk-M202, Tomsk-M83, Tomsk-K6, Novosibirsk-L2008, C11-13 and 886-84 strains and cells were obtained from a collection of SRC VB "Vector" (Novosibirsk, Russia). Viral strains were propagated on PEK (pig embryonic kidney) cells before sequencing as described previously [22]. Additionally, C11-13 TBEV was cultivated on Neuro-2a and 293 cells for 6 to 7 passages.

RNA isolation and sequencing

The isolation of the total RNA was performed from the infected cell lysates. For this purpose, 10 volumes of TRIzol® Reagent (Invitrogen Corporation, USA) were added to the cell samples, and the samples were incubated at 65 °C for 15 min; then, 300 µl of chloroform was added, and the aqueous phase was extracted. The aqueous phase was washed with 300 µl of chloroform and was transferred to a new tube. Then, 500 µl of cooled isopropanol and 1 µl glycogen were added to the tube. The RNA sample was centrifuged at 20,000×*g* for 15 min at 4 °C, and the isolated RNA was washed with 70% ethanol.

The cDNA synthesis was carried out with 5′-d(N)6-3′ oligonucleotides using the Reverta-L kit (Moscow, Russia). The mixture was incubated for 1 min at 95 °C and was placed in an ice bath; then, a mixture containing M-MulV was added. The cDNA synthesis was performed for 1 h at 37 °C. The PCR amplification of the TBEV fragments was carried out using a set of primers described previously [23]. The sequencing of the isolated PCR fragments was performed using an ABI 3130xl genetic analyser according to the manufacturer's instructions.

Modelling 3′ UTR genomic RNA

Multiple alignments of the 3′ UTR TBEV sequences were performed using Lasergene 9. The secondary structures of the 3′ UTR TBEV were predicted using the MFOLD 3.4 server. The maximum distance between the base pairs and the suboptimal percent has been selected manually. The RNA conformations that were predicted in the stem-loop (SL) and Y-shaped structures were annotated based on the level of homology after aligning the nucleotide sequences.

Results

The sequencing and size characterization of the full-length genome for different strains of TBEV

Twenty-two TBEV strains were sequenced for the characterization of their complete genomes, and the strain C11-13 was adapted from human brain cells to 293 cells, Neuro-2a cells and PEK cells. Phylogenetic analysis showed that these strains have been divided into the three major subtypes of TBEV (Fig. 1). Ten strains were classified as TBEV-FE, and these strains were isolated from samples collected in Siberia and from the Far Eastern region of Russia from 1937 to 2008. Seven strains were typed as TBEV-Sib, and these strains were isolated in Central Asia and Western Siberia from 1986 to 2013. The

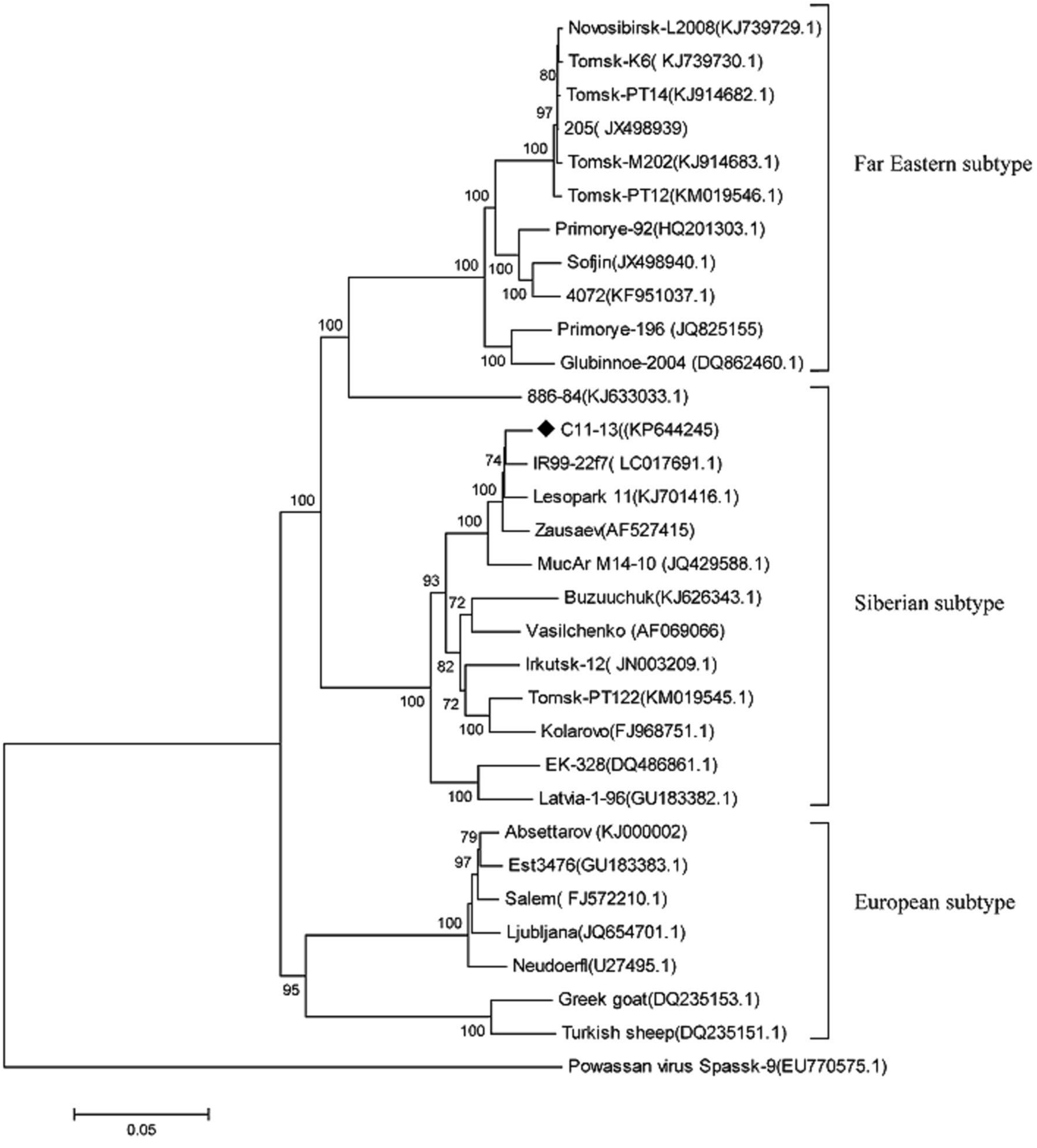

Fig. 1 The phylogenetic tree for the complete genomic TBEV sequences. Phylograms were constructed with the neighbour-joining method with MEGA 5. The bootstrap value is shown when it is > 70%. The Powassan virus was used as an outgroup. The significance of the constructed tree was estimated by bootstrap analysis with 1000 replicates. The GenBank accession numbers are given in parentheses

European subtype is presented by the Absettarov strain (Karelia, 1951). C11-13 TBEV-Sib and its variants were obtained by adaptation to different cell cultures and were grouped together with other strains in the Siberian subtype (Fig. 1). The early strain 886-84 TBEV (EF469662) was isolated in the Irkutsk region in 1984 and was classified as a putative Baikalian subtype of TBEV [24, 25]. Resequencing (KJ633033) showed that the 886-84 TBEV genome was longer than previously defined by 160 nucleotides. Based on the genome organization features, the 3′ UTR and the genome size of this strain are closer to the Siberian subtype and may be classified as a separate group from that of TBEV-Sib.

The results of the comparison of the complete genomes and the 3′ UTR sizes are presented in Table 1. Almost all complete genomes for the three main subtypes of TBEV under cultivation in identical laboratory conditions had different sizes. The Absettarov strain of TBEV-Eu is the longest genome (11,097 nucleotides). The smallest genome size is characteristic for all strains of TBEV-FE; for example,

Table 1 The comparison of the length for genomic RNAs and 3′ UTRs of TBEV

Strain, GenBank	Complete genome	Variable region 3′ UTR	Conserved region 3′ UTR	Full 3′ UTR
European subtype				
Absettarov, KJ000002	11,097	402	321	723
Salem, FJ572210	11,068	403	312	715
Neudoerfl, U27495	11,141	446	321	767
Hypr_IC, KP716974	11,103	407	322	729
KrM93, HM535611[a]	11,097	402	321	723
Length (nucleotides)	11,068–11,141	402–446	312–322	715–767
Siberian subtype				
Kolarovo-2008, FJ968751	10,928	232	321	553
Zausaev, AF527415	10,832	138	320	458
Vasilchenko, AF069066	10,927	233	320	553
Lesopark11, KJ701416	10,886	182	320	502
Buzuuchuk, KJ626343	10,923	229	320	549
C11-13, KP644245	10,802	107	321	428
C11-13PAK, MF043953	10,838	144	320	464
C11-13-293, MF043954	10,823	129	320	449
C11-13-Neu, MF043955	10,839	144	321	465
Tomsk–PT122, KM019545	10,933	413	146	576
Length (nucleotides)	10,802–10,933	107–413	146–321	428–576
Baikalian subtype of TBEV[b]				
886-84, KJ633033	10,916	222	320	542
Far Eastern subtype				
Glubinnoe/2004, DQ862460	10,886	201	312	513
4072, KF951037	10,894	201	320	521
205, JX498939	10,495	67	55[c]	122[c]
Sofjin, JX498940	10,894	201	320	520
Tomsk-PT12, KM019546	10,780	92	320	512
Tomsk-PT14, KJ914682	10,780	87	320	508
Tomsk-M202, KJ914683	10,780	92	320	512
Tomsk-M83, KJ739731	10,785	87	325	507
Tomsk-K6, KJ739730	10,776	87	316	503
Novosibirsk-L2008, KJ739729	10,771	87	312	499
Length (nucleotides)	10,495–10,894	67–201	312–325	499–521

The TBEV strains that were sequenced by the authors are indicated in bold

[a] The TBEV-Eu strain KrM 93 was isolated in South Korea from the lung tissues of wild rodents (*Apodemus agrarius*) in 2006

[b] The TBEV strain 886-84 was isolated from the Irkutsk region in 1984 and was proposed to be a putative Baikalian subtype of TBEV

[c] Incomplete sequences of the C3′ UTRs

the genome of Novosibirsk-L2008 has only 10,771 nucleotides. Additionally, a comparison of the published complete genome sequences (GenBank) for 18 strains of the TBEV-Eu subtype, 55 strains of the Siberian subtype and 71 strains of the Far Eastern subtype has shown that the average size of the TBEV genome differs by approximately 100 nucleotides. The strains of TBEV-Eu have the largest genome length, and the strains of TBEV-FE have the shortest genome length.

Heterogeneity of the 3′ UTR of the viral genome

Significant heterogeneity of the V3′ UTR of the TBEV genome, which varies from 87 to 446 nucleotides, is influenced by the viral genome size (Table 1). The size of the V3′ UTR of the TBEV-Eu subtype ranged from 402 to 446 nucleotides, and for the TBEV-FE subtype, it was only 67–201 nucleotides. Aligning the 3′ UTRs showed that the longest 3′ UTR sequences are typical for the Absettarov and Neudoerfl strains that belong to the European subtype (Fig. 2). Neudoerfl also has a short polyA sequence that is actually missing from the other TBEVs. Usually, the C3′ UTR remains unchanged, and 3′ UTR deletions have been found in the polyA to polyC regions of the V3′ UTR. The formation of a Y-shaped structure is also predicted in this region.

A non-aligned region (NAR) was found for Tomsk-PT122 TBEV-Sib (Fig. 2). Because of the additional insertion, the V3′ UTR size is increasing by up to 413 nucleotides (Table 1). The NAR in the V3′ UTR of Tomsk-PT122 is completely formed by nucleotide insertions from the coding regions of viral protein E and NS4a. The NAR putative scheme of arrangement for the three homologous fragments that have a ≥ 70% level of identity from the protein E and NS4a gene fragments (24–26 nucleotides) are shown in Fig. 2.

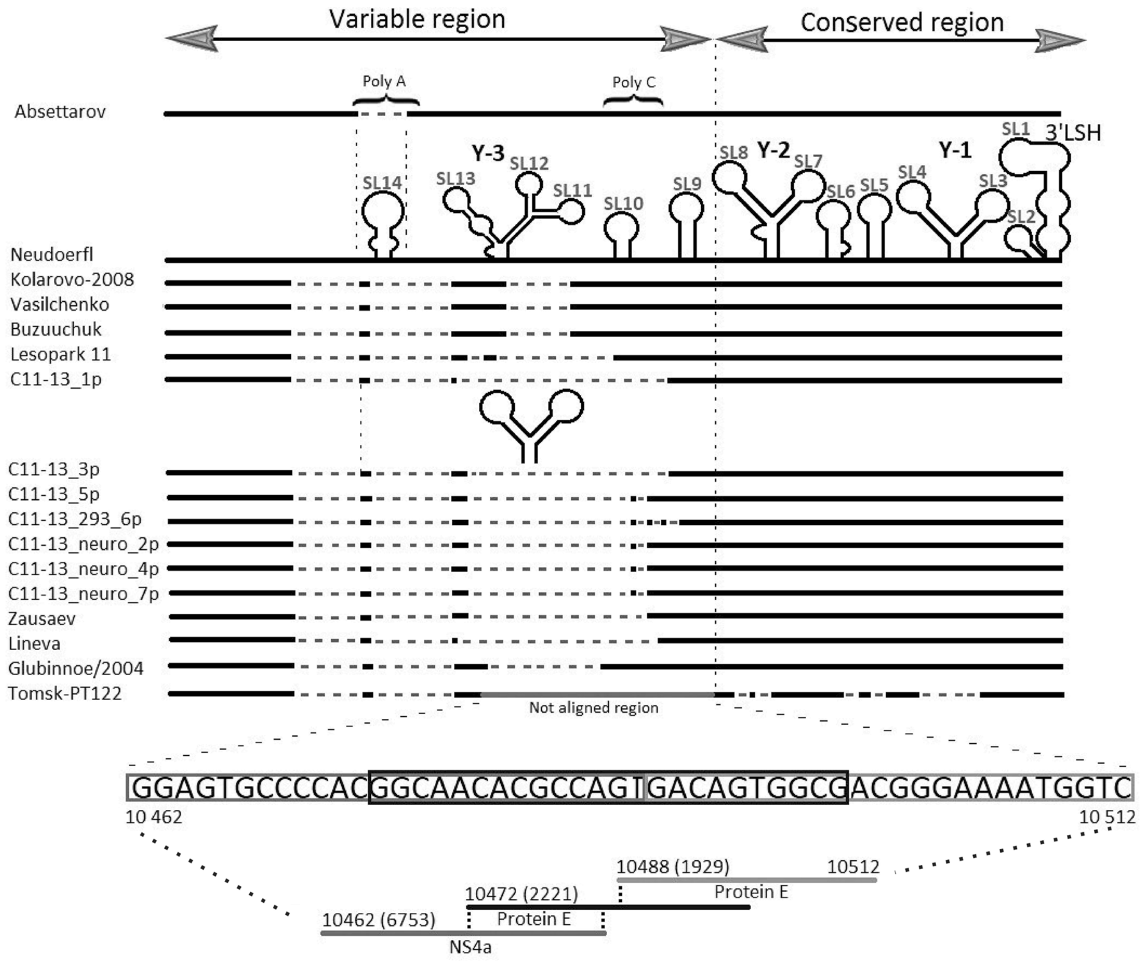

Fig. 2 The scheme of the full-size 3′ UTR nucleotide sequence alignment. The secondary structures of the 3′ UTR are schematically presented for the Neudoerfl strain of TBEV, and this is the strain that has the longest genome. The alignment is presented in this order: European, Siberian and Far Eastern subtypes. The TBEV-Sib strain Tomsk-PT122 is presented separately (last line) because this strain has an unusual 3′ UTR structure

Modelling the secondary structure of the 3′ UTR RNA of TBEV

The conserved sequences of TBEV and other flaviviruses were used as anchors for the alignment of the 3′ UTR sequences (Fig. 2). The RNA secondary structure was simulated for the 3′ UTR genomic RNA of the 3 major subtypes of TBEV (Fig. 3). The most complex secondary structure of the 3′ UTR has been found in TBEV-Eu. This genotype has the largest genome size (~ 11,100 n.) and the V3′ UTR length ranges from 100 to 200 nucleotides, which is greater than those of the other TBEV subtypes. The available SL9, SL10 and Y-3 structures located in the V3′ UTR have been characterized for TBEV-Eu. Moreover, the strain KrM 93, the additional Y-4 structure has been predicted, unlike other TBEV-Eu strains. The SL14 and SL15 structures in the V3′ UTRs of the Neudoerfl and Hypr_IC TBEV-Eu strains are formed instead of the Y-4 structure.

TBEV-Sib and TBEV-FE have structural similarities for their V3′ UTRs, unlike the European subtype. The V3′ UTRs of these subtypes consists of several Y-shaped structures. An additional SL with Y-shaped structures is predicted with the increasing length of the 3′ UTR; for example, Y-3 structures are modified by SL9, SL10, SL11, SL12 and SL13 in the Kolarovo-2008 TBEV-Sib strain. Among the TBEV-FE strains, the V3′ UTR Tomsk-M202 represented the only Y-4 structure located near NS5, which may be induced by a deletion within 100 nucleotides of the V3′ UTR.

The V3′ UTRs of TBEVs have significant differences depending on the subtype. The RNA secondary structures of the C3′ UTRs of TBEVs include the promoter that is formed by a conserved long stem-loop designated as 3′ LSH that is divided by SL1 and SL2 as described previously [17]. A very conservative pentanucleotide sequence CACAG is located on top of the SL1 of the 3′ UTR of TBEV. We found that only Tomsk-PT122 has an unusual 3′ LSH with reduced levels of SL1 and a completely modified SL2. The pentanucleotide sequence AACAU is the basis for SL1 formation, and it is another possible putative sequence of the viral promoter. Additionally, the hexanucleotide sequence UUGGCA in SL3 interacts with the inverted repeat sequence UGCCAA on top of SL6, which may be a principal for the RNA secondary structure of the TBEV promoter.

The enhancer is mapped early between the stop codon and the promoter [17]. This region is also formed by the C3′ UTR and the V3′ UTR sequences (Figs. 2, 3). The length of the enhancer greatly varied between the different TBEV subtypes. The analysis of the RNA secondary structures of this region showed that Y-like structures are typical for TBEV enhancers. The more complex Y-like structures are predominant within the Siberian subtype.

Variability of the V3′ UTR in new types of host cells

The Tomsk-PT122 and Kolarovo-2008 strains of the TBEV-Sib subtype were directly isolated from different hosts: Blyth's Reed Warbler *(Acrocephalus dumetorum)* and Ixodes tick (*Ixodes pavlovskyi*). The geographical sites of the isolation of these strains, the time and the phylogenetic groups are very close. Earlier, these stains were classified as putative TBEV recombinants by 7 recombination detection algorithms [26]. It is interesting that the 3′ UTRs are also modified (Figs. 2, 3). The Y-3 located V3′ UTR for both strains has a very complex secondary structure. The length of the V3′ UTR of Tomsk-PT122 is 413 nucleotides, which is the maximum size within the TBEV-Sib subtype (Table 1). The putative scheme of insertions of the short fragments (24–26 nucleotides) of E and the NS4a viral genes into the V3′ UTR of Tomsk-PT122 is presented in Fig. 2. The elongation of the V3′ UTR for Tomsk-PT122 may be the first direct evidence of intragenomic RNA modification (insertions) for TBEV-Sib.

The 3′ LSH of Tomsk-PT122 is also strongly modified (Fig. 3d). The stem-loops SL1 and SL2 also disappear. The pentanucleotide sequence AACAU is the base for SL1 instead of the flaviviral conservative pentanucleotide sequence CACAG. Additionally, the C3′ UTR of Tomsk-PT122 has several deletions of approximately 170 nucleotides in length (Fig. 2).

During the adaptation of C11-13 TBEV-Sib to 293, PEK and Neuro-2a cells also showed an increased V3′ UTR length from 107 to 144 nucleotides (Fig. 2). This leads to the modification of Y-3 in LRS 4 and the size of these fragments, which has increased in all C11-13 variants derived from all three types of cells. Moreover, the increasing sizes of the 3′ UTRs are 21 (293 cells), 36 (PEK cells) and 37 (Neuro-2a cells) nucleotides.

Discussion

The 3′ UTRs of TBEVs are divided into the C3′ UTR and the V3′ UTR, which includes the 6 LRSs typical of other flaviviruses [6, 10]. Additionally, the 3′ UTR may be subdivided into promoters and enhancers. The promoter contains the region that is required for RNA replication and for ensuring the infectious activity of TBEV. The experimentally determined TBFV promoter corresponded roughly to the 3′ LSH-SL2Y-shaped structure. The region between the stop codon and the promoter is defined as the enhancer region and is not critical for the infectivity of TBEV. Nevertheless, it has been suggested that the variability of the 3′ UTR flaviviral genome is related to the variability of the promoter and/or enhancer as a mechanism for flaviviral adaptation to different cells of vertebrate and invertebrate hosts [10]. In all

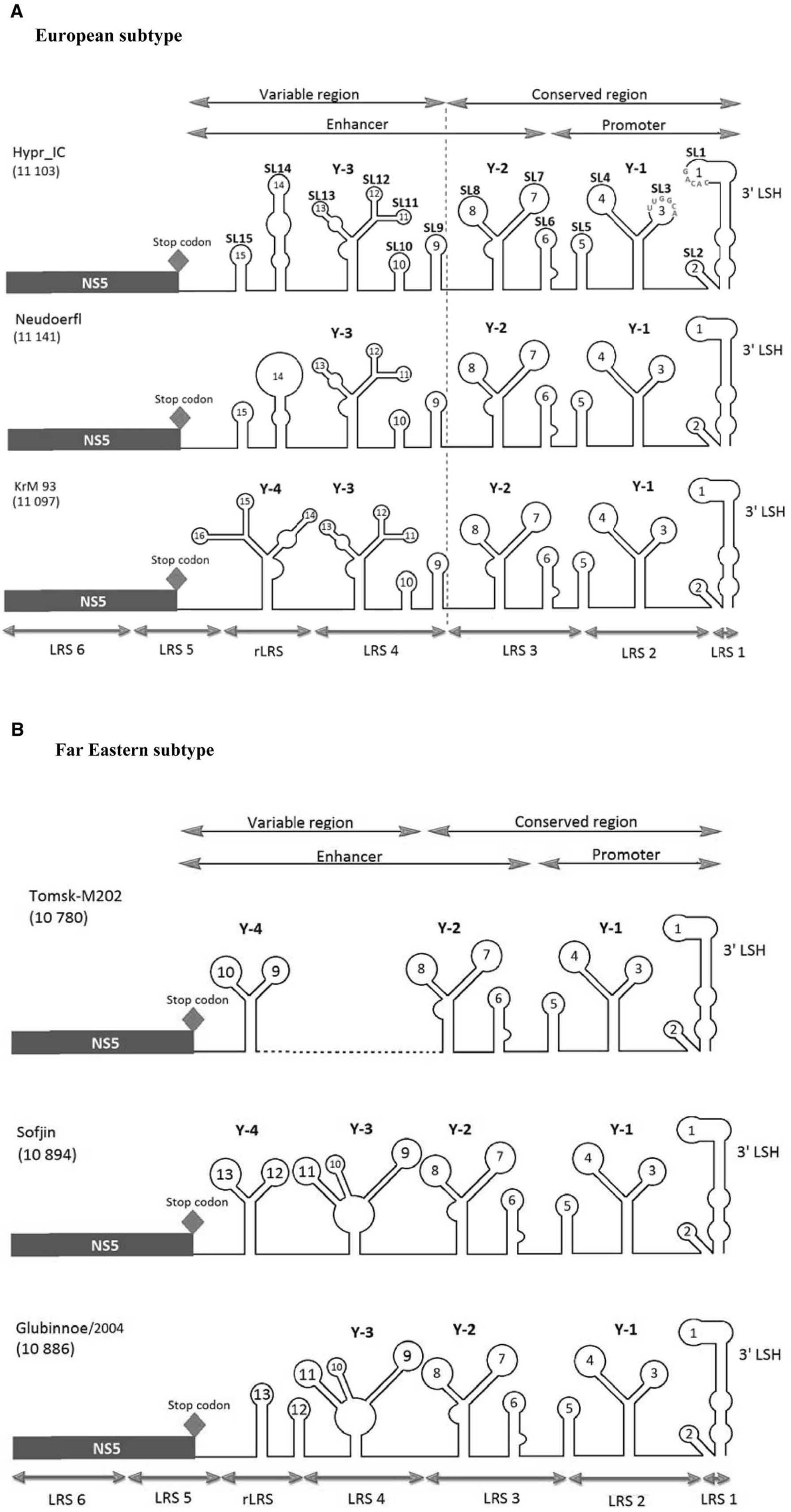

Fig. 3 Linear model of the secondary structures of the 3′ UTRs of TBEV-Eu (**a**), TBEV-FE (**b**), TBEV-Sib (**c**) and the Tomsk-PT122 strain of TBEV-Sib (**d**). This model was built using the server MFOLD (http://unafold.rna.albany.edu/?q=mfold/RNA-Folding-Form)

Fig. 3 (continued)

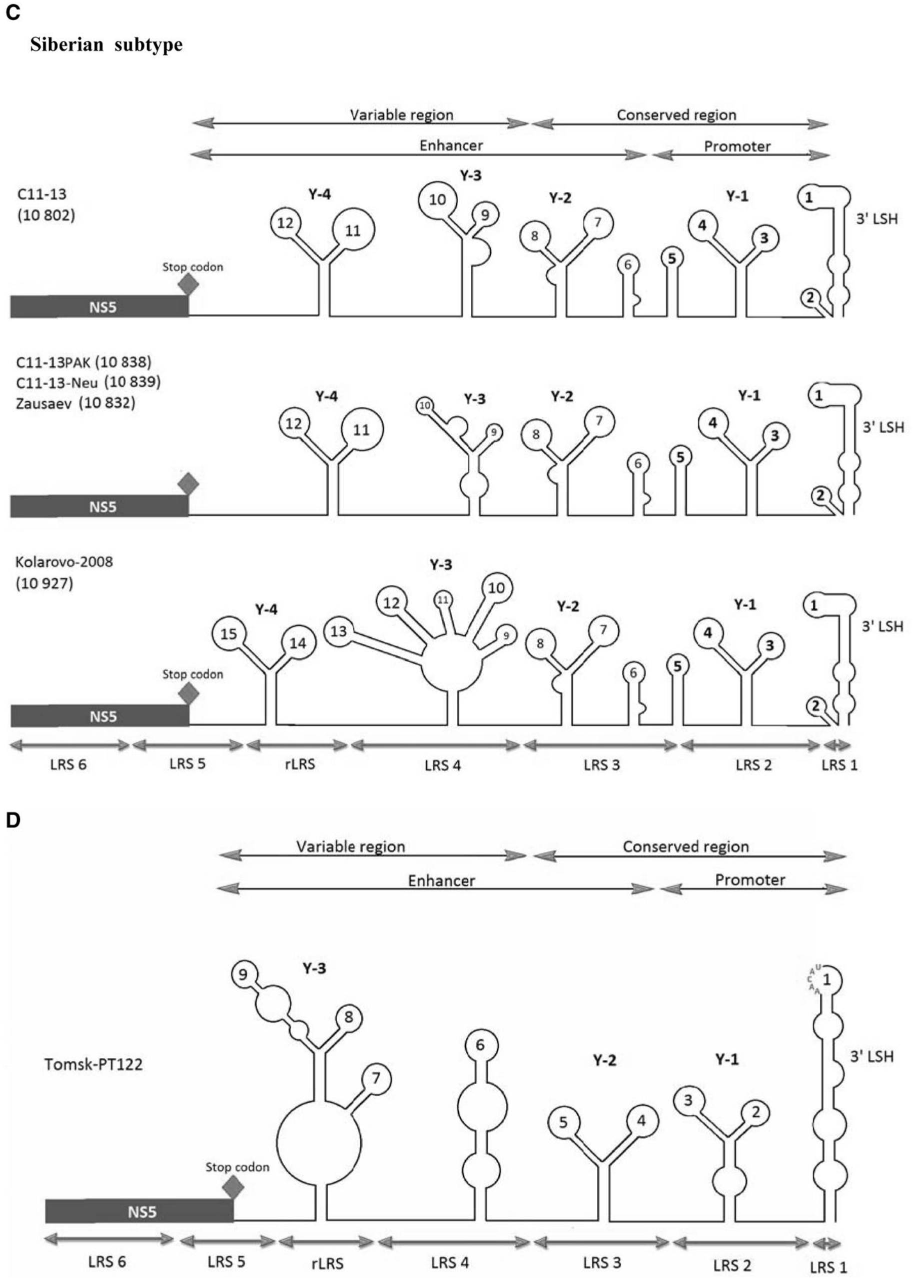

likelihood, the enhancer may not be critical to ensure infectious virus activity in experimental conditions but may be crucial to the transmission of the virus between the vector and susceptible hosts, thereby ensuring the success of flavivirus survival in different natural foci and climatic zones.

It has been suggested that TBFV originally had 9 LRS [10]. Subsequently, the TBFV group completely lost three LRS proximally close to a stop codon. This region is not essential for the viability of TBEV [9]. Most likely, the poly-AT sequence appeared in the early stages of flavivirus evolution. This is based on the fact that polyA has been detected in MBFV, and it was possibly formed as a result of RNA-dependent RNA polymerase activity [10]. Conserving poly-AT in some flaviviruses probably reflects the need to maintain a selective advantage for flaviviruses in nature.

The analysis of the complete genomes of the 3 major TBEV subtypes revealed that TBEV-Eu has longer genomes, and the smallest genome size is typical for TBEV-FE. A major role in the length of the viral genome is the significant heterogeneity of the V3′ UTR, which ranged from 67 to 446 nucleotides. The size of the V3′ UTR for TBEV-Eu ranged from 402 to 446 nucleotides, and that of the TBEV-FE ranged from 67 to 201 nucleotides.

Our modelling 3′ UTR TBEV revealed changes in RNA secondary structure mainly in the variable region. The most conserved region of the 3′ UTR for all TBEV genotypes is the 3′ LSH. It was also found that the V3′ UTR has typical differences for the TBEV subtype. The more complex RNA structure of the V3′ UTR has been discovered for TBEV-Eu, which includes a double Y-shaped structure and 2–4 SLs. TBEV-FE has 1 or 2 Y-shaped structures in the V3′ UTR, and TBEV-Sib usually has two Y-shaped structures. The Tomsk-PT122 strain that was isolated from birds has only 1 SL and 1 double Y-shaped structure in the V3′ UTR and has a significantly modified structure in the 3′LSH C3′ UTR. This strain also has the largest genome size among TBEV-Sib.

Earlier, several isolates of C11-13 TBEV-Sib were selected during passages into PEK, 293 and Neuro-2a cells [22]. The amino acid substitutions were found in the NS1, NS2a, NS3 and NS5 polypeptides. Additionally, the variable length of the V3′ UTR was discovered for the C11-13 isolates. During passages C11-13 into PEK, 293 and Neuro-2a cells, the length of the V3′ UTR increased from 107 to 144 nucleotides. These modifications induced the Y-shaped structure of LRS 4 in different types of cells. Another opinion suggests that the length of the V3′ UTR of TBEV may be changed during the replication of TBEV into new cell types. The elongation V3′ UTR for Tomsk-PT122 and the laboratory variants of C11-13 proposed an insertion of additional RNA fragments. Insertions have been found in the V3′ UTR of Tomsk-PT122 with short fragments (24-26 nucleotides) of the E and NS4a viral genes. Early, the putative recombination sites are located in the regions of the E and NS4 genes, especially in the NS4 gene [27]. We evaluated that the elongation of the V3′ UTR for Tomsk-PT122, which was isolated from birds, and C11-13, which was isolated from humans, is the first direct evidence of intragenomic RNA recombination (insertions) for TBEV-Sib subtypes and are possible for other TBFVs. We can assume that the observed features for the 3′ UTRs of the laboratory strains of TBEV after multiple passages in cell cultures are primarily due to the adaptation to laboratory cultivation.

In all likelihood, the mechanism for changing the 3′ UTR is fundamentally important for effective TBEV replication into the cells of different hosts. The large sizes of the V3′ UTR of TBEV-Eu and their genomes allow us to hypothesize that the dissemination of TBEV in Eurasia could be from the West to the East. The variability of the 3′ UTRs of RNAs is the principal for the replication and enhancement of the survival strategy for TBEVs in different hosts in the ever-changing natural and climatic conditions.

Acknowledgements The authors would like to gratefully acknowledge support from the Russian Federal Service for Surveillance on Consumer Rights Protection and Human Wellbeing (GZ for SRC VB “Vector” № 141-00069-18-01 from 17.03.2018).

Author contributions VAT and VBL conceived and designed the experiments and wrote the manuscript. AVG and ANS performed the experiments and analysed the data and assisted in writing the manuscript. EPP performed the experiments and assisted in the writing of manuscript. TMP, EVA, SNK and EVC performed the experiments.

Compliance with ethical standards

Conflict of interest The authors declare that there is no conflict of interest. No competing financial interests exist.

Research involving human participants and/or animals The present study did not involve any human subject or animal.

Informed consent The present study did not involve any human subject and therefore, no need of informed consent.

References

1. Grard G, Moureau G, Charrel RN, Lemasson JJ, Gonzalez JP, Gallian P, Gritsun TS, Holmes EC, Gould EA, de Lamballerie X (2007) Genetic characterization of tick-borne flaviviruses: new insights into evolution, pathogenetic determinants and taxonomy. Virology 361:80–92. https://doi.org/10.1016/j.virol.2006.09.015
2. Gritsun TS, Lashkevich VA, Gould EA (2003) Tick-born encephalitis. Antiviral Res 57:129–146
3. Gritsun TS, Venugopal K, Zanotto PM, Mikhailov MV, Sall AA, Holmes EC, Polkinghorne I, Frolova TV, Pogodina VV, Lashkevich VA, Gould EA (1997) Complete sequence of two tick-borne flaviviruses isolated from Siberia and the UK: analysis and significance of the 5′ and 3′ UTRs. Virus Res 49:27–39
4. Proutski V, Gritsun TS, Gould EA, Holmes EC (1999) Biological consequences of deletions within the 3′-untranslated region of flaviviruses may be due to rearrangements of RNA secondary structure. Virus Res 64:107–123
5. Markoff L (2003) 5′- and 3′-noncoding regions in flavivirus RNA. Adv Virus Res 59:177–228
6. Gritsun TS, Gould EA (2006) The 3′ untranslated region of tick-borne flaviviruses originated by the duplication of long repeat sequences within the open reading frame. Virology 350:269–275. https://doi.org/10.1016/j.virol.2006.03.002
7. Thurner C, Witwer C, Hofacker IL, Stadler PF (2004) Conserved RNA secondary structures in Flaviviridae genomes. J Gen Virol 85(Pt 5):1113–1124. https://doi.org/10.1099/vir.0.19462-0
8. Men R, Bray M, Clark D, Chanock RM, Lai CJ (1996) Dengue type 4 virus mutants containing deletions in the 3’ noncoding region of the RNA genome: analysis of growth restriction in cell culture and altered viremia pattern and immunogenicity in rhesus monkeys. J Virol 70:3930–3937
9. Mandl CW, Aberle JH, Aberle SW, Holzmann H, Allison SL, Heinz FX (1998) In vitro-synthesized infectious RNA as an attenuated live vaccine in a flavivirus model. Nat Med 4(12):1438–1440. https://doi.org/10.1038/4031
10. Gritsun TS, Gould EA (2006) Direct repeats in the 3’ untranslated regions of mosquito-borne flaviviruses: possible implications for virus transmission. J Gen Virol 87(Pt 11):3297–3305. https://doi.org/10.1099/vir.0.82235-0
11. Hahn CS, Hahn YS, Rice CM, Lee E, Dalgarno L, Strauss EG, Strauss JH (1987) Conserved elements in the 3’ untranslated region of flavivirus RNAs and potential cyclization sequences. J Mol Biol 198:33–41
12. Charlier N, Leyssen P, Pleij CW, Lemey P, Billoir F, Van Laethem K, Vandamme AM, De Clercq E, de Lamballerie X, Neyts J (2002) Complete genome sequence of Montana

Myotis leukoencephalitis virus, phylogenetic analysis and comparative study of the 3’ untranslated region of flaviviruses with no known vector. J Gen Virol 83(Pt 8):1875–1885. https://doi.org/10.1099/0022-1317-83-8-1875

13. Pletnev AG (2001) Infectious cDNA clone of attenuated Langat tick-borne flavivirus (strain E5) and a 3’ deletion mutant constructed from it exhibit decreased neuroinvasiveness in immunodeficient mice. Virology 282:288–300. https://doi.org/10.1006/viro.2001.0846
14. Chausov EV, Ternovoi VA, Protopopova EV, Kononova JV, Konovalova SN, Pershikova NL, Romanenko VN, Ivanova NV, Bolshakova NP, Moskvitina NS, Loktev VB (2010) Variability of the tick-borne encephalitis virus genome in the 5’ noncoding region derived from ticks Ixodes persulcatus and Ixodes pavlovskyi in Western Siberia. Vector Borne Zoonotic Dis 10:365–375. https://doi.org/10.1089/vbz.2009.0064
15. Ecker M, Allison SL, Meixner T, Heinz FX (1999) Sequence analysis and genetic classification of tick-born encephalitis viruses from Europe and Asia. J Gen Virol 80:179–185. https://doi.org/10.1099/0022-1317-80-1-179
16. Ternovoi VA, Protopopova EV, Chausov EV, Novikov DV, Leonova GN, Netesov SV, Loktev VB (2007) Novel variant of tickborne encephalitis virus, Russia. Emerg Infect Dis 13:1574–1578. https://doi.org/10.3201/eid1310.070158
17. Gritsun DJ, Jones IM, Gould EA, Gritsun TS (2014) Molecular archaeology of Flaviviridae untranslated regions: duplicated RNA structures in the replication enhancer of Flaviviruses and Pestiviruses emerged via convergent evolution. PLoS ONE. https://doi.org/10.1371/journal.pone.0092056
18. Wallner G, Mandl CW, Kunz C, Heinz FX (1995) The flavivirus 3’-noncoding region: extensive size heterogeneity independent of evolutionary relationships among strains of tick-borne encephalitis virus. Virology 213:169–178. https://doi.org/10.1006/viro.1995.1557
19. Sakai M, Yoshii K, Sunden Y, Yokozawa K, Hirano M, Kariwa H (2014) Variable region of the 3’ UTR is a critical virulence factor in the Far-Eastern subtype of tick-borne encephalitis virus in a mouse model. J Gen Virol 95(Pt 4):823–835. https://doi.org/10.1099/vir.0.060046-0
20. Sakai M, Muto M, Hirano M, Kariwa H, Yoshii K (2015) Virulence of tick-borne encephalitis virus is associated with intact conformational viral RNA structures in the variable region of the 3’-UTR. Virus Res 203:36–40. https://doi.org/10.1016/j.virusres.2015.03.006
21. Muto M, Kamitani W, Sakai M, Hirano M, Kobayashi S, Kariwa H, Yoshii K (2018) Identification and analysis of host proteins that interact with the 3’-untranslated region of tick-borne encephalitis virus genomic RNA. Virus Res 249:52–56. https://doi.org/10.1016/j.virusres.2018.03.006
22. Ponomareva EP, Ternovoi VA, Mikryukova TP, Protopopova EV, Gladysheva AV, Shvalov AN, Konovalova SN, Chausov EV, Loktev VB (2017) Adaptation of tick-borne encephalitis virus from human brain to different cell cultures induces multiple genomic substitutions. Arch Virol 162:3151–3156. https://doi.org/10.1007/s00705-017-3442-x
23. Chausov EV, Ternovoy VA, Protopopova EV, Konovalova SN, Kononova Yu V, Tupota NL, Moskvitina NS, Romanenko VN, Ivanova NV, Bol’shakova NP, Leonova GN, Loktev VB (2011) Molecular genetic analysis of the complete genome of tick-borne encephalitis virus (Siberian subtype): modern Kolarovo-2008 isolate. Probl Part Danger Infect 110:44–48 (**in Russian**)
24. Demina TV, Dzhioev IuP, Kozlova IV, Verkhozina MM, Tkachev SE, Doroshchenko EK, Lisak OV, Paramonov AI, Zlobin VI (2012) Genotypes 4 and 5 of the tick-borne encephalitis virus: features of the genome structure and possible scenario for its formation. Vopr Virusol 57(4):13–19 (**in Russian**)
25. Dai X, Shang G, Lu S, Yang J, Xu J (2018) A new subtype of eastern tick-borne encephalitis virus discovered in Qinghai-Tibet Plateau, China. Emerg Microbes Infect 7(1):74. https://doi.org/10.1038/s41426-018-0081-6
26. Bertrand YJ, Johansson M, Norberg P (2016) Revisiting recombination signal in the tick-borne encephalitis virus: a simulation approach. PLoS ONE. https://doi.org/10.1371/journal.pone.0164435
27. Dzhioev YP, Paramonov A, Reva ON, Bukin YS, Kozlova IV, Demina TV, Tkachev SE, Zlobin VI (2015) Detection of potential sites of recombination in the tick-borne encephalitis virus by the methods of comparative genomics. Vopr Virusol 60(3):44–49 (**in Russian**)